Shape Control of Alloy Steel Rolled by Sendzimir Mill

J. T. Kim*, J. J. Yi* and S. Y. Han**

(Received July 18, 1995)

In order to improve quarter waves occurred in the wide and thin gauged alloy steel rolled by 20-high sendzimir mill, a computer simulation based on the divided element method and an actual cold rolling experiment were carried out. Quarter waves were simulated by elastic deformation analysis of rolls considering bending deformation of back up rolls and the effect of control actuators on controllability of quarter waves were analyzed. Computer simulation showed that control actuators such as shifting of the 1st intermediate roll and crown adjustment of As-U-Roll in back up rolls were not effective to control quarter waves and that changing taper mode (both length and magnitude) at the barrel-end taper radius of the 1st intermediate roll was rather very effective. From an actual rolling experiment it was verified that quarter waves could be reduced remarkerably by changing taper mode of the 1st intermediate roll.

Key Words: Sendzimir Mill, Shape Control, Quarter Wave, Shifting, Taper, 1st Intermediate Roll (IMR), As-U-Roll

1. Introduction

Sendzimir mill is widely used for rolling hard materials such as stainless, silicon and alloy steels. It is composed of small diameter of work rolls for reducing rolling load and many rolls for backing up the work rolls. As shape control actuators, there are shifting of the 1st intermediate roll (IMR) in the width direction of strip, taper mode (length and magnitude) of the 1st IMR and crown adjustment of As-U-Roll in back up rolls (BUR). But since sendzimir mill has small diameter of work rolls in comparison with 4-high and 6-high mills, quarter waves are occurred at quarter part of strip by complex elastic deformations of work rolls. It results in a large obstacle of shape quality and productivity.

Generally, design for taper mode of the 1st IMR has been considered as the most effective method to control strip shape and it has been determined by experience and experiments. However, taper mode of the 1st IMR currently used is not sufficient to control quarter waves occurred by various rolling conditions. Therefore, an analytic approach to shape analysis of sendzimir mill in order to optimal taper mode of the 1st IMR is necessary. Hattori (1984), Mizuta (1987) and Matsuda (1987) have been studied for elastic deformation analysis of rolls of sendzimir mill based on the divided element model by assuming BUR to be rigid body or considering bending of BUR. But little study of reducing quarter waves has been done until now and although Hara (1991) has suggested a concave mode of the 1st IMR, it is not pratical because of accuracy of roll grinding.

In this paper, quarter waves were simulated by roll deformation analysis of sendzimir mill considering bending deformation of BUR and the effect of control actuators of sendzimir mill on controllability of quarter waves were analyzed and then an effective method to reduce quarter waves was accomplished. Finally, the effect of the developed method was verified by an actual rolling experiment.

* Research Institute of Science and Technology P. O. Box 135, Pohang, Korea, 790-600

** Department of Automotive Engineering, Hanyang Univ. 17, Haengdang-Dong, Seongdong-Ku, Seoul, Korea

2. Method of Solution

2.1 Elastic deformation analysis

2.1.1 Modelling

The roll arragement of sendzimir mill is shown in Fig. 1 and the divided element method suggested by Shohet and Boyce (1968) was applied for elastic deformation analysis of rolls. The assumptions used for analysis were as follows :

a. Rolling is symmetric with respect to x- and y-axis so that only quarter part of the system needs to be analyzed.

b. Tension distribution in the width direction is constant.

c. Contact angles in the width direction between rolls are constant.

d. Contact pressure at each divided element is constant.

The divided number in the width direction of rolls was m and the deformation of As-U-Roll was given compulsorily at each saddle position as shown in Fig. 2.

(1) Equilibrium equations

As shown in Fig. 3, the Nth roll applied by q numbers of distributed loads was considered. IF $P_x^N(j)$ and $P_y^N(j)$ are sums of x- and y-direction forces applied at the Nth roll, respectively, they can be written as follows.

$$P_x^N(j)=\sum_{k=1}^{q}\{\cos\theta_k\cdot P_k^N(j)\} \tag{1}$$

$$P_y^N(j)=\sum_{k=1}^{q}\{\sin\theta_k\cdot P_k^N(j)\} \tag{2}$$

where, j and θ_k indicate divided element index and contact angle, respectively.

- Equilibrium equations of forces for the Nth roll (roll ①, ②, ③ and ④)

$$\sum_{j=1}^{m}\{P_x^N(j)\cdot\triangle W(j)\}=0 \tag{3}$$

$$\sum_{j=1}^{m}\{P_y^N(j)\cdot\triangle W(j)\}=0 \tag{4}$$

where, $\triangle W(j)$ is divided element length.

- Equilibrium equations of moments for the Nth roll (roll ①, ②, ③ and ④)

$$\sum_{j=1}^{m}\left\{P_x^N(j)\cdot\triangle W(j)\cdot\frac{UL(j)}{RL}\right\}=0 \tag{5}$$

$$\sum_{j=1}^{m}\left\{P_y^N(j)\cdot\triangle W(j)\cdot\frac{UL(j)}{RL}\right\}=0 \tag{6}$$

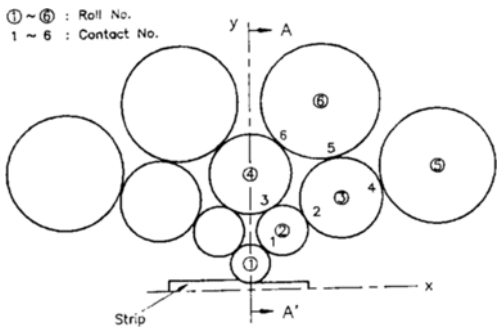

Fig. 1 Roll arrangement of sendzimir mill

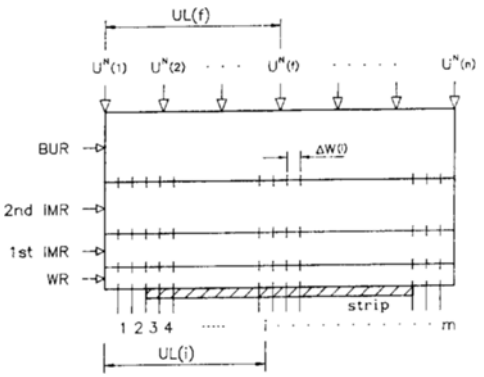

Fig. 2 Analysis model of roll deflection based on divided element method

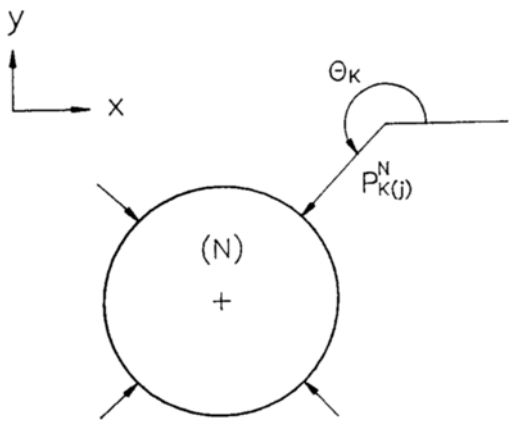

Fig. 3 Force equilibrium of roll

where, RL is roll length and $UL(j)$ is the distance from left end to the jth element.

- Equilibrium equations of forces for the Nth roll (roll ⑤ and ⑥)

$$\sum_{j=1}^{m} P_x^N(j)\cdot\triangle W(j)-\sum_{k=1}^{n} R_x^N(K)=0 \tag{7}$$

$$\sum_{j=1}^{m} P_y^N(j)\cdot\triangle W(j)-\sum_{k=1}^{n} R_y^N(K)=0 \tag{8}$$

where, $R_x^N(K)$ and $R_y^N(K)$ indicate the reaction forces in the x- and y-direction of BUR, respectively.

- Equilibrium equations of moments for the Nth roll (roll ⑤ and ⑥)

$$\sum_{j=1}^{m} P_x^N(j)\cdot\triangle W(j)\frac{UL(j)}{RL} - \sum_{k=1}^{n} R_x^N(K)\cdot\frac{UL(K)}{RL}=0 \tag{9}$$

$$\sum_{j=1}^{m} P_y^N(j)\cdot\triangle W(j)\frac{UL(j)}{RL} - \sum_{k=1}^{n} R_y^N(K)\cdot\frac{UL(K)}{RL}=0 \tag{10}$$

(2) Deformations of rolls

The influence coefficients $a(i, j)$'s, which mean the deformation at the center of the ith element when unit distribution load (Mizuta, 1987) as shown in Fig. 4 is applied at the jth element due to bending considering shear force, can be represented by the following equations.

(a) $0\le x<a$

$$a(i,j)=\frac{-1}{48EI}\left\{\frac{8f}{L}(x^3-L^2x)+x\left(\frac{8f^3}{L}-\frac{2bc^2}{L}+\frac{c^3}{L}+2c^2\right)\right\}+\frac{16}{3\pi GD^2}\cdot\frac{fx}{L} \tag{11}$$

(b) $a<x\le b$

$$a(i,j)=\frac{-1}{48EI}\left\{\frac{8f}{L}(x^3-L^2x)+x\left(\frac{8f^3}{L}-\frac{2bc^2}{L}+\frac{c^3}{L}+2c^2-\frac{2(x-a)^4}{c}\right)\right\}+\frac{16}{3\pi GD^2}\left\{\frac{fa}{L}+\frac{f(x-a)}{L}-\frac{x^2-a^2}{2c}+\frac{ax-a^2}{c}\right\} \tag{12}$$

(c) $b<x\le a$

$$a(i,j)=\frac{-1}{48EI}\left\{\frac{8}{L}(L-f)[(L-x)^3-L^2(L-x)]+(L-x)\left[\frac{8}{L}(L-f)^3-\frac{2(L-b+c)c^2}{L}+\frac{c^3}{L}+2c^2\right]\right\}+\frac{16}{3\pi GD^2}\cdot\frac{(L-f)(L-x)}{L} \tag{13}$$

where,

D : Roll diameter.

I : The moment of inertia of the cross-sectional area

E : Young's modulus of roll.

G : Shear modulus of elasticity of roll

In the case that roll M is contacted with roll N by contact angle θ_A at the point A and the roll N is applied by q numbers of distributed loads as shown in Fig. 5, the deformations of roll N in the x- and y-dirction can be obtained as follows.

- For rolls ①, ②, ③ and ④

$$Y_x^N(i)=\sum_{j=1}^{m} a^N(i,j)\cdot P_x^N(j)\cdot\triangle W(j)$$

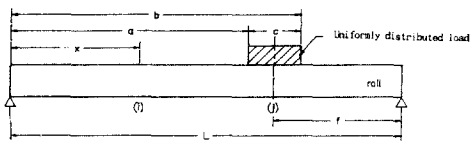

Fig. 4 Roll idealized as a cantilever beam

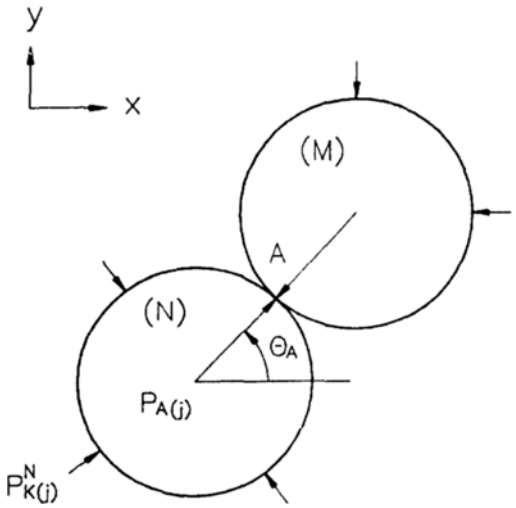

Fig. 5 Contact between rolls

$$-\frac{UL(i)}{RL}(K_{xL}^N-K_{xR}^N)+K_{xL}^N \tag{14}$$

$$Y_y^N(i)=\sum_{j=1}^{m}\alpha^N(i,\ j)\cdot P_y^N(j)\cdot\triangle W(j)-\frac{UL(i)}{RL}(K_{yL}^N-K_{yR}^N)+K_{yL}^N \tag{15}$$

- For rolls ⑤ and ⑥

If K_{xL}^N and K_{xR}^N represent the displacements in the x-direction of BUR shown in Fig. 2 at $UL(f)=0$ and $UL(f)=RL$, respectively, displacement $U_x^N(f)$ for $f=2\sim(n-1)$ in the x-direction can be written by the following equation (Mizuta, 1982).

$$U_x^N=\sum_{j=1}^{m}\alpha^N(f,\ j)\cdot P_x^N(j)\cdot\triangle W(j)+\sum_{K=1}^{n}\alpha^N(f,\ K)\cdot R_x^N(K)-\frac{UL(f)}{RL}(K_{xL}^N-K_{xR}^N)+K_{xL}^N \tag{16}$$

Then, $R_x^N(1)$ and $R_x^N(n)$ can be obtained by use of Eqs. (7) and (9).

$$R_x^N(1)=\sum_{j=1}^{m}P_x^N(j)\cdot\triangle W(j)\cdot\left(1-\frac{UL(j)}{RL}\right)-\sum_{K=1}^{n}R_x^N(K)\cdot\left(1-\frac{UL(K)}{RL}\right) \tag{17}$$

$$R_x^N(n)=\sum_{j=1}^{m}P_x^N(j)\cdot\triangle W(j)\cdot\frac{UL(j)}{RL}-\sum_{K=1}^{n}R_x^N(K)\cdot\frac{UL(K)}{RL} \tag{18}$$

By substituting Eqs. (17) and (18) into Eq. (16), $U_x^N(f)$ for $f=2\sim(n-1)$ can be represented as follows.

$$U_x^N(f)=\sum_{j=1}^{m}P_x^N(j)\cdot\triangle W(j)\left\{\alpha^N(f,\ j)+\alpha^N(f,\ 1)\left(1-\frac{UL(j)}{RL}\right)+\alpha^N(f,\ n)\frac{UL(J)}{RL}\right\}-\sum_{K=2}^{n-1}R_x^N(K)\cdot\left\{\alpha^N(f,\ 1)\left(1-\frac{UL(K)}{RL}\right)+\alpha^N(f,\ n)\frac{UL(K)}{RL}-\alpha^N(f,\ K)\right\}-\frac{UL(f)}{RL}(K_{xL}^N-K_{xR}^N)+K_{xL}^N \tag{19}$$

Eq. (19) can be represented by a matrix form.

$$(U_x^N)^*=[M_1]^*(P_x^N)-[M_2]^*(R_x^N)^*-[M_3]^*(K_{xL}^N-K_{xR}^N)+[M_4]^*(K_{xL}^N) \tag{20}$$

where, $*$ indicates $f=2\sim(n-1)$. $(R_x^N)^*$ can be obtained by multipling the inverse matrix of $[M_2]^*$ by both sides of Eq. (20). Then, $R_x^N(1)$ and $R_x^N(n)$ can be expressed in a matrix form.

$$R_x^N(1)=(N_1)^t(P_x^N)-(N_2)^{*t}(R_x^N)^* \tag{21}$$

$$R_x^N(n)=(N_3)^t(P_x^N)-(N_4)^{*t}(R_x^N)^* \tag{22}$$

If we set $K_{xL}^N=U_x^N(1)$ and $K_{xR}^N=U_x^N(n)$, (R_x^N) is expressed for $f=1\sim n$ as follows.

$$(R_x^N)=[G_1](P_x^N)+[G_2](U_x^N) \tag{23}$$

Then, the deformation $Y_x^N(i)$ in the x-direction for the ith element becomes

$$Y_x^N(i)=\sum_{j=1}^{m}\alpha^N(i,\ j)\cdot P_x^N(j)\cdot\triangle W(j)+\sum_{K=1}^{n}\alpha^N(i,\ K)\cdot R_x^N(K)-\frac{UL(i)}{RL}(K_{xL}^N-K_{xR}^N)+K_{xL}^N \tag{24}$$

If Eq. (23) is substituted into Eq. (24), $Y_x^N(i)$ can be obtained in a matrix form as follows and $Y_y^N(i)$ can be obtained by the similar method.

$$(Y_x^N)=[Q_1](P_x^N)+[Q_2](U_x^N) \tag{25}$$

Now, $Y_x^N(i)$ and $Y_y^N(i)$ for $f=1\sim n$ are summarized in terms of the divided element.

$$Y_x^N(i)=\sum_{j=1}^{m}\alpha^{*N}(i,\ j)\cdot P_x^N(j)\cdot\triangle W(j)+\sum_{f=1}^{n}\beta^N(i,\ f)\cdot U_x^N(f) \tag{26}$$

$$Y_y^N(i)=\sum_{j=1}^{m}\alpha^{*N}(i,\ j)\cdot P_y^N(j)\cdot\triangle W(j)+\sum_{f=1}^{n}\beta^N(i,\ f)\cdot U_y^N(f) \tag{27}$$

where, $\alpha^{*N}(i,\ j)$ and $\beta^N(i,\ f)$ are related with the elements of (P_x^N), (P_y^N), (U_x^N) and (U_y^N).

(3) Compatibility equations

The deformation in the θ_A-direction $Y_{\theta A}^N(i)$ of the Nth roll can be expressed by

$$Y_{\theta A}^N(i)=Y_x^N(i)\cos\theta_A+Y_y^N(i)\sin\theta_A \tag{28}$$

from Fig. 5 and the deformation in the θ_A-direction $Y_{\theta A}^M(i)$ of the Mth roll can be obtained in a similar manner. By using Eq. (28), the following compatibility equations in the θ_A-direction between roll N and M were obtained.

$$Y_{\theta A}^{N}(i) - Y_{\theta A}^{M}(i) - C^{N}(i) - C^{M}(i) = -P_{A}(i)/KU(i) \quad (29)$$

where

$C^{N}(i)$: Magnitude of crown and taper of the Nth roll

$C^{M}(i)$: Magnitude of crown and taper of the Mth roll

$KU(i)$: Spring constant between roll N and M

$P_{A}(i)$: Contact pressure between roll N and M

(4) Total matrix of the system

By using the equations of equilibrium and compatibility, total matrix of the system can be written as follows.

$$[A](P) = [A_1](F) + [A_2](S') + [A_3](S) + [A_4](C) + [A_5](U_x) + [A_6](U_y) \quad (30)$$

where,

(P) : Load vector per unit width at contact point of rolls

(F) : Load vector per unit width applied at work roll

(S') : Skew-symmetric rigid displacement vector of each roll

(S) : Symmetric rigid displacement vector of each roll

(C) : Vector of roll crown and taper

(U_x, U_y) : Displacement vector at the support point of back up roll

where, $[A]$ and $[A_4]$ are 6 m$\times$6 m, $[A_1]$ is 6m$\times$ m, $[A_2]$ and $[A_3]$ are 6m$\times$8, $[A_5]$ and $[A_6]$ are 6m$\times 2n$ matrices, respectively. By solving Eq. (30), contact loads at each contact point are determined and then the deformation of each roll can be calculated by them.

(5) Flattening between work roll and strip

Work roll is flattened by cantact pressure between work roll and strip, which directly affect the thickness profile at exit. In this analysis, it is calculated by use of the solution for elastic half-space problem based on two dimensional contact theory (Yamamoto, 1982 and Tozawa, 1970).

(6) Spring constants for contact rolls

Spring constants measured for between solid rolls or between solid roll and BUR in sendzimir mill by Hattori (1984) were used in this analysis.

2.1.2 Computer simulation

Simulation program was prepared for calculating strip thickness profile by use of inputs of material conditions such as strip width, a kind of steels and hot coil profile, of operation conditions such as reduction ratio, tension and roll crown and of equipment conditions such as diameters and positions of rolls and shifting of 1st IMR. The program was composed of input, calculation of rolling force, calculation of influence coefficients, matrix composition and solver, contact condition handling and output.

In this analysis, rolling force was calculated by Brand & Ford (1948)'s equation and then after the influence coefficients were calculated, total matrix of the system was composed in order to determine contact loads for each roll. In calculations, if some of the contact loads came out negative, total matrix of the system were recomposed after setting the negative values to zero for those elements. From the determined contact loads, rigid displacements, rolling forces, flattening between work roll and strip and displacement of work roll, thickness profile of the strip was obtained. In calculations, thickness at the strip center was always maintained as target thickness at exit and strip thickness profile was calculated by relative displacements with respect to thickness at strip center. This calculation was iterated until the difference of elongation for the last divided element of the strip between the previous and current calculation was within 1/50000.

The flow chart of calculation is shown in Fig. 6. The roll dimensions used for calculation are summarized in Table 1, and 3-step taper mode of 1st. IMR is shown in Fig. 7, and the dimensions are shown in Table 2. And rolling conditions for simulation of STS304 are shown in Table 3. Finally, the crown pattern of As-U-Roll is shown in Table 4, where crown in the negative y-direction is indicated by positive value.

2.2 Principle of shape measurement

Two sets of shapemeter are being equipped each at the entry and the exit of sendzimir mill, which are used for measurement of strip shape by measuring average tension deviation at each section of the strip. Shapemeter is consisted of several divided rolls in the width direction of roll as shown in Fig. 8. The outer surface of each divided roll is a shell type and four transducers under the each shell are equipped at 90 degree spacing. Hence, contact load Fi due to contact between roll and strip is measured 4 times per revolution. Average tension deviation at each divided roll can be calculated by Eq. (31) using the measured contact load Fi. Also, average strain deviation can be used for measurement of strip shape by $\sigma = E\varepsilon$(E : Young's modulus of strip, ε : strain in the rolling direction), so that the shape of strip can be measured either average tension deviation or average strain deviation.

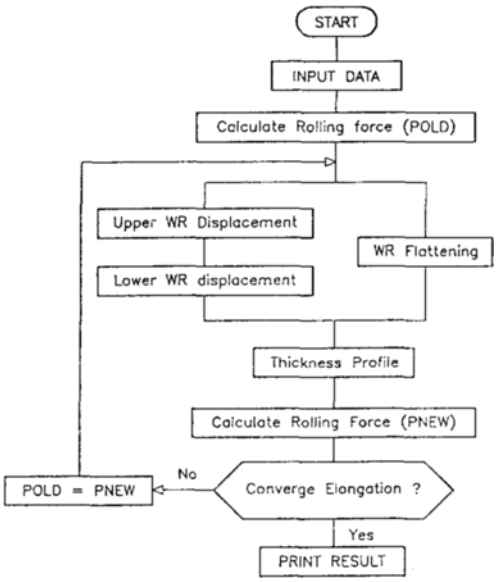

Fig. 6 Flow chart of calculating thickness profile

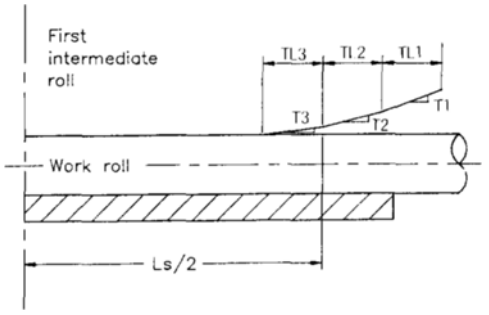

Fig. 7 Taper of the 1st IMR

Table 1 Rolldimensions used for calculation

Roll Type	Diameter(mm)
Work Roll	90
1st IMR	137.4
2nd IMR(drive)	230.7
2nd IMR(idle)	232.0
Back-up bearing	406.1

Table 2 Dimensions of 3-step taper of 1st IMR for rolling

(unit : mm)

Taper	1st Step Taper(T1)	20./20000
	2nd Step Taper(T2)	6.7/20000
	3rd Step Taper(T3)	2.5/20000
Taper length	TL1	350
	TL2	185
	TL3	144

Table 3 Rolling conditions (STS304)

Strip width	1270 mm
Hot coil thickness	3.11 mm
Strip thickness(entry)	0.86 mm
Strip thickness(exit)	0.76 mm
Front tension	40 kg/mm^2
Back tension	36 kg/mm^2
Amount of shift(upper)	106.0 mm
Amount of shift(lower)	106.0 mm

Table 4 As-U-Roll crown pattern (unit : mm)

Type	#1	#2	#3	#4	#5	#6	#7	#8
A	0.18	0.091	- 0.136	0.0	0.0	−0.136	0.091	0.18
B	0.18	0.091	−0.317	0.0	0.0	−0.317	0.091	0.18

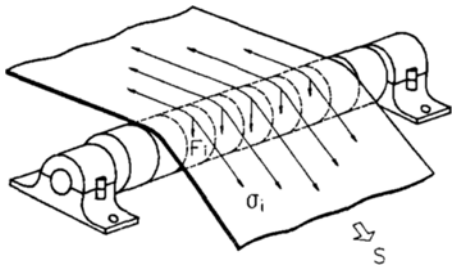

Fig. 8 Schematic diagram of shapemeter

$$\triangle\sigma_i=\frac{F_i-\bar{F}}{F_i}\frac{S}{tw} \tag{31}$$

where, $\bar{F}=(1/n)\sum_{i=1}^{n}F_i$

$\bar{F}$: Average contact load

F_i : Contact load at the i-th divided roll

n : The number of the divided rolls

$\triangle\sigma_i$: Average tension deviation at the i-th divided roll

S : Total tension

t : Strip thickness

w : Strip width

Quarter waves are often occurred in the case of wide width of strip (above 1000 mm), for example, if the width of strip is assumed to be 1200 mm, quarter waves are occurred around at 300 mm and 900 mm from the edge. In this case, average tension deviation $\triangle\sigma_i$ at the quarter part of the strip shows lower value than the other part due to large elongation of the quarter part.

3. Results and Discussions

3.1 Simulation results and discussions

Computer simulation for reducing the quarter waves of the strip under the actual rolling conditions shown in Table 3 was carried out by following the calculation flow of strip thickness profile shown in Fig. 6. In order to examine the validity of computer simulation program, elongation in the width direction of strip measured by shapemeter was compared with that calculated by computer simulation program. Comparison result is shown in Fig. 9. It showed a good agreement and also regenerated a tendency of quarter waves.

Then, the effect of control actuators such as taper length, taper magnitude and shifting of the

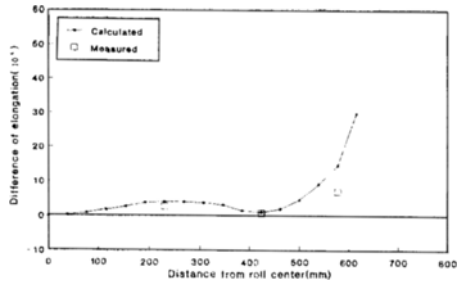

Fig. 9 Comparison between measured and calculated thickness profile

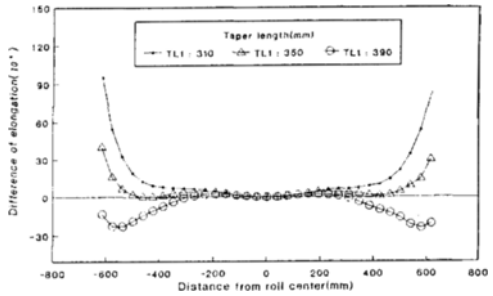

Fig. 10 Effect of the first taper length(TL1) of the 1st IMR on quarter waves

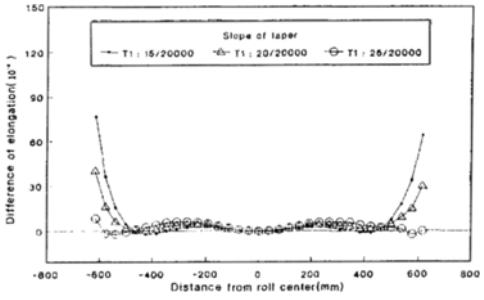

Fig. 11 Effect of the first taper magnitude(T1) of the 1st IMR. on quarter waves

1st IMR and crown adjustment of As-U-Roll of sendzimir mill on controllability of quarter waves were examined. Figure 10 shows the effect of the first taper length $TL1$ on quarter waves. When $TL1$ was larger than the current taper length, quarter waves were almost not changed and elongation at strip edge became smaller so that average tension at strip edge became larger. In contrast, when $TL1$ was smaller than the current taper length, quarter waves were disappered but large edge waves were occurred. Hence, it was concluded that taper length $TL1$ was not effective

on improvement of quarter waves. Figure 11 shows the effect of the fist taper magnitude $T1$ on quarter waves. When $T1$ was changed either larger or smaller than the current taper magnitude, quarter waves were almost not changed and only elongation at strip edge was changed. Thus, it was found that taper magnitude $T1$ was not effective on reducing of quarter waves. The similar simulation results for $TL2$, $TL3$, $T2$ and $T3$ were obtained as above. The effect of the shifting of the 1st IMR on quarter waves was examined. The result is shown in Fig. 12. When the shifting of the 1st IMR was changed either larger or smaller than the current shifting of the 1st IMR, the quarter waves were almost not changed. It was found that the shifting of the 1st IMR was not effective on reducing of the quarter waves. Also the effect of crown adjustment of As-U-Roll on the quarter waves was examined. B-type of As-U-Roll crown pattern shown in Table 4 was compared with A-type of the current As-U-Roll crown pattern and the result is shown in Fig. 13. It showed that quarter waves were regenerated, so that it was not effective on improving quarter waves.

Next, in order to find a way to improve quarter waves, computer simulation was carried out by changing both taper length and taper magnitude simultaneously. As shown in Fig. 14, $TL2$(185 → 165 mm), $TL3$(144 → 244 mm) and $T3$(2.5/20000 → 1.8/20000) were found as optimal values of taper length and taper magnitude of the 1st IMR (new taper) and the values of the other control actuators were used the same as current rolling conditions (old taper). From Fig. 14, it was found that quarter waves were improved signicantly. Contact force in the width direction between work roll and the 1st IMR is shown in Fig. 15 and it showed the comparison of currently used (old) taper and optimal (new) taper of the 1st IMR for contact force. It was found that contact force at the quarter part of strip was reduced and conversely that at about −400 mm was increased, in the case of new taper comparing with old taper. It affected deformation of work roll, so that quarter waves could be controlled effectively. The fact that the values of contact

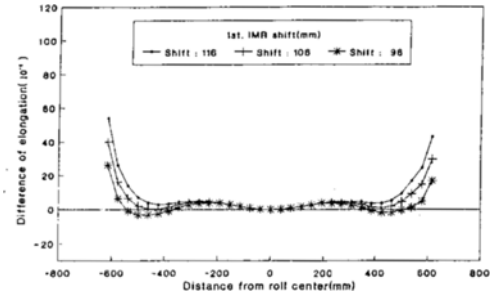

Fig. 12 Effect of the shifting of the 1st IMR on quarter waves

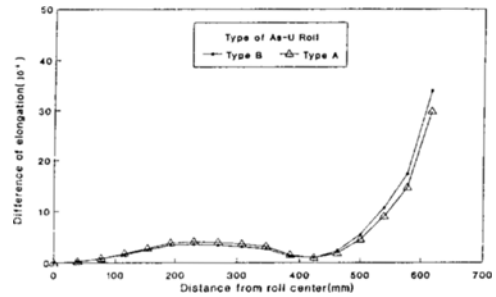

Fig. 13 Effect of the crown adjustment of As-U-Roll on quarter waves

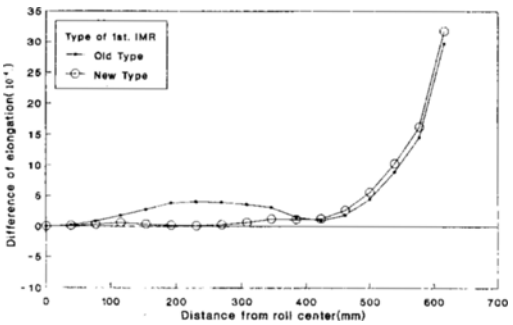

Fig. 14 Effect of the optimal(new) taper of the 1st IMR on quarter wavens

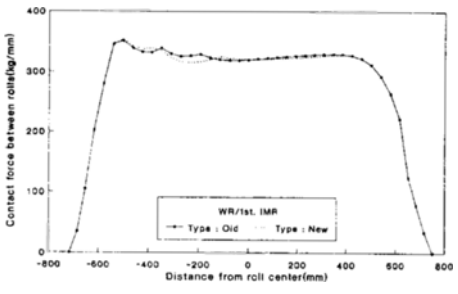

Fig. 15 Effect of new taper of the 1st IMR on inter-roll contact force

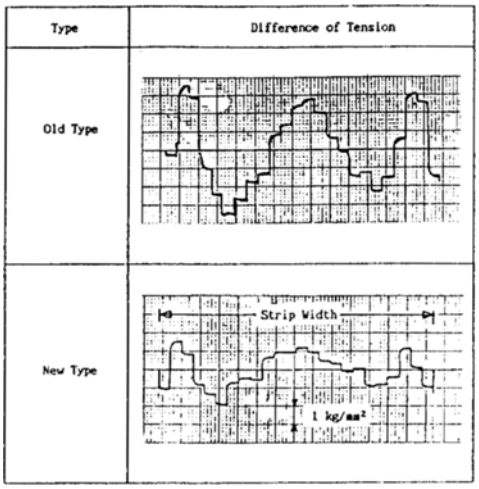

Fig. 16 Result of the test rolling

pressure were antisymmetric with respect to center of strip is due to the structure of sendzimir mill, that is, since taper of the 1st IMR is made in one side only, the structure of sendzimir mill lies in point-symmetry with respect to center of it.

3.2 Application in an actual plant

In order to verify the effect of new taper of the 1st IMR on quarter waves, an experiment for comparing old taper with new taper under actual rolling conditions was carried out by rolling several strips of 3.12^t at entry and $0.68^t \times 1265^w$ at exit for STS304. Average tension diffences between old taper and new taper after rolling were compared shown in Fig. 16. From the experiment result, average tension difference for old taper was about $\pm 3.5\ kg/mm^2$ and for new taper was about $\pm 1.9\ kg/mm^2$. Therefore, it was confirmed that new taper of the 1st IMR was very effective on improvement of quarter waves.

4. Conclusions

The following conclusions have been obtained from computer simulations and an actual rolling experiment for reducing quarter waves of stainless steel rolled by sendzimir mill.

(1) Computer simulations have been succesfully made for regenerating quarter waves of strip rolled by sendzimir mill throughout elastic deformation analysis of rolls.

(2) By examining the effect of control actuators such as taper length, taper magnitude and shifting of the 1st IMR and crown adjustment of As-U-Roll of sendzimir mill on controllability of quarter waves, one concluded that it was not effective on reducing quarter waves of strip when each control actuator mentioned above was applied independently.

(3) It was confirmed that only optimal taper modified by changing both taper length and magnitude of the 1st IMR was very effective on improvement of quarter waves analytically and experimentally.

References

Bland D. R. and Ford, H., 1948, "The Calculation of Roll Force and Torque in Cold Strip Rolling with Tensions," *Proc. Inst. Mech. Eng.*, Vol. 158, pp. 174.

Hara K., 1991, "Shape Controllability for Quarter Buckles of Strip in 20-high Sendzimir Mills," *ISIJ*, Vol. 31, No. 6, pp. 607~613.

Hattori S., 1984, "Effects of Roll Arragements and Roll Sizes on Shape Controllability of Cluster Mills," *Advanced Tech. of Plasticity*, Vol. 2, pp. 1230~1235.

Matsuda, T., 1987, "An Analysis of Roll Deformation of Sendzimir Mill," *Proc. 4th Intl. Steel Rolling Conf.*, Vol. 2, pp. E.39.

Mizuta, A., 1982, "Analysis of Roll Deflection in a Twenty-High Mill," *J. Jap. Soc. Tech. Plasticity*, Vol. 23, No. 163, pp. 1245~1252.

Mizuta, A., 1987, "Characteristics of Shape Control of Multi-High Mill," Vol. 28, No. 321, pp. 1042~1047.

Shohet, K. N. and Boyce, M. F., Nov., 1968, "Static Model Tests of Roll Bending Methods of Crown Control," *J. Iron and Steel Inst.*, Vol. 206, pp. 1088~1102.

Tozawa, Y., 1970,"Analysis to Obtain the Pressure Distributions from the Contuour of Deformed Roll," *J. Jap. Soc. Tech. Plasticity*, Vol. 11, No. 108, pp. 29.

Yamamoto, 1982, "Shape Control of Plate at Z-high Mill," *J. Jap. Soc. Tech. Plasticity*, Vol. 23, No. 263, pp. 1267.